Cu-O network dependent core hole screening in low-dimensional cuprate systems: a high-resolution x-ray photoemission study

T. Böske, K. Maiti[a], O. Knauff, K. Ruck, M. S. Golden, G. Krabbes, and J. Fink
Institut für Festkörper- und Werkstofforschung Dresden, Postfach 270016, 01171 Dresden, Germany

T. Osafune, N. Motoyama, H. Eisaki, and S. Uchida
Department of Superconductivity, Faculty of Engineering, University of Tokyo, Yayoi 2-11-16, Bunkyo-ku, Tokyo 113, Japan

Abstract

We present an experimental study of the dynamics of holes in the valence bands of 0, 1, and 2 dimensional undoped model cuprates, as expressed via the screening of a Cu 2*p* core hole. The response depends strongly upon the dimensionality and the details of the Cu-O-Cu network geometry and clearly goes beyond the present theoretical state-of-the-art description within the three-band *d*-*p* model.

74.72.Jt, 71.27.+a, 74.25.Jb

The dynamics of single hole states in low dimensional, highly correlated electron systems are currently of great interest in the context of the high-T_C superconducting cuprates. Recently, the band dispersion of a single hole in an antiferromagnetic insulator consisting of a two-dimensional (2D) Cu-O network has been studied[1] and has promoted further investigations in this direction.[2,3] As regards one-dimensional (1D) CuO_2 chain systems, a separation between spin and charge excitations most unlike the planar CuO_2 systems has recently been reported in the zigzag chain cuprate $SrCuO_2$.[4]

The application of core level x-ray photoemission spectroscopy (XPS) to study the electronic structure of correlated systems is widely established, and from an analysis of their Cu $2p$ core level line shapes important contributions to the understanding of the electronic structure of the high-T_C cuprates have been derived.[5] Experimentally, the Cu $2p$ photoelectron spectra of the formally divalent copper compounds show a so-called satellite emission at higher binding energy than a broad asymmetric main line. Such spectra can be approximately described with cluster calculations[6] or in an Anderson impurity model[5,7] using only one Cu site. These single-site models discriminate between poorly screened multiplets of the $2p^5 3d^9$ final state, mainly responsible for the satellite and a well screened $2p^5 3d^{10}\underline{L}$ final state for the main line emission, where $\underline{L}$ denotes that the intrinsic valence band hole is situated in the ligands surrounding the Cu $2p$ core hole site. The energy separation and the intensity ratio of these spectral features are determined by the valence band-core hole interaction energy U_{dc}, the effective Cu $3d$-O $2p$ hopping energy t, and the charge transfer energy between a Cu $3d$ and an O $2p$ state Δ.[6] However, the experimentally observed large width and asymmetry of the Cu $2p$ main line could not be understood within these models.

To tackle this problem, the single-site models have been extended to include different sites within the Cu-O network by considering larger clusters.[8] For a linear Cu_3O_{10} cluster, the Cu $2p$ main line was predicted to consist of two components:[8] the lowest binding energy feature would be due to a so-called nonlocal screening process where the valence band hole delocalizes to form a Zhang-Rice singlet (ZRS) state on CuO_4 plaquettes other than where the core hole resides. The higher binding energy component would then be a final state where the valence band hole is predominantly located in the O $2p$ states immediately surrounding the core hole site and is consequently called a locally screened final state. In order to calculate the Cu $2p$ XPS of larger systems (such as infinite chains or planes) further approximations have to be made.[9] Such calculations appear to show, however, that in general there remain considerable cluster-size dependencies in the results. For example, the prominent double-featured main line predicted for the linear Cu_3O_{10} cluster[8] appears to be absent in larger 1D and 2D systems.[9] This is in agreement with previous Cu $2p$ photoemission data of different cuprates where no double feature in the main line has been reported,[10,11] but it disagrees with a recent study of $Sr_2CuO_2Cl_2$ where the Cu $2p$ main line is shown to consist of at least three distinct features.[12]

Therefore, a complete study of the Cu $2p$ photoemission as a function of both the dimensionality and the Cu-O-Cu interaction geometry is needed to put the multiple-site models on a sound basis and to directly verify the different screening channels experimentally. Furthermore, based upon the multiple-site screening approach, XPS offers an elegant way to study the dynamics of hole states in different Cu-O networks. In this paper we present the first systematic study of Cu $2p$ photoemission in various undoped cuprates with 0, 1, and 2D Cu-O networks. In particular, using high-resolution XPS, we examine high-quality single-crystals of Bi_2CuO_4, Li_2CuO_2, $Ba_3Cu_2O_4Cl_2$, Sr_2CuO_3, $SrCuO_2$, $Sr_2CuO_2Cl_2$, and $Ba_2Cu_3O_4Cl_2$. These systems together represent a wide variety of Cu-O network structures as depicted in Fig. 1.

For the 1D systems, we study the extreme Cu-O-Cu interaction angles, ranging from 180° in the linear chain Sr_2CuO_3 to nearly 90° in Li_2CuO_2. Both of these limiting Cu-O-Cu configurations play a defining role in the physics of the spin-ladder systems[13] which are currently of great interest. We also include Bi_2CuO_4 in this study as a representative of a so-called zero-dimensional (0D) system. In this compound, the CuO_4 plaquettes are stacked along the c direction with O-Bi-O bridging units[14] and no coherent Cu-O network is realized. $Ba_3Cu_2O_4Cl_2$ contains chains of edge-shared CuO_4 plaquettes, which are so arranged as to give a crenellated Cu-O network as depicted in Fig. 1.[15]

$Sr_2CuO_2Cl_2$ is considered to be the paradigm 2D spin-$\frac{1}{2}$ Heisenberg antiferromagnet.[16] $Ba_2Cu_3O_4Cl_2$ has a similar structure to that of $Sr_2CuO_2Cl_2$,[17] although its Cu-O network is composed of a regular CuO_2 plane (denoted by Cu_A in Fig. 1) with an additional Cu site (Cu_B) which is connected to the regular Cu_AO_2 plane via a 90° Cu_A-O-Cu_B configuration. Consequently, the Cu atoms in $Ba_2Cu_3O_4Cl_2$ show two antiferromagnetic phase-transitions at widely different temperatures and two different ZRS dispersion functions connected with these different Cu sub-systems.[3]

The experiments were carried out using a Perkin-Elmer photoemission system equipped with a monochromatic Al Kα source giving a resolution of about 0.4 eV. Since the samples are insulating, corrections for charging effects were undertaken resulting in an estimated accuracy of the given absolute energy values of ±0.3 eV. The measurements were performed at room temperature and the crystals were cleaved *in situ* under ultrahigh vacuum conditions. The O 1s spectra of all samples show negligible emission at binding energies greater than 531 eV, which indicates clean samples. We found that the shape of the Cu 2p spectra depends critically on the cleanliness of the oxygen signal.

In Fig. 2 we show the Cu $2p_{\frac{3}{2}}$ spectra of the cuprates. An integral background has been subtracted and the spectra are normalized to the leading peak. The area of the $Ba_2Cu_3O_4Cl_2$ spectrum is multiplied by a factor of 1.5 compared to that of $Sr_2CuO_2Cl_2$, assuming it to be proportional to the number of Cu atoms in the Cu-O plane for reasons to be shown later. The spectral features for all crystals studied are summarized in Table I.

In the following, we will describe the salient features of the Cu 2p main lines and then discuss the role of the electronic states near the chemical potential in the screening processes responsible for the observed structures. In contrast to all previous XPS studies known to us, the Cu 2p main line spectra show either a rich fine structure or are fairly narrow symmetric lines. The position of the lowest binding energy feature denoted by A is the same within our experimental accuracy for all the systems studied. The spectrum of Bi_2CuO_4 is very similar to a previously published one.[18] A recent low resolution XPS study also gave a comparable spectrum for polycrystalline Sr_2CuO_3,[11] although, in the present case using high resolution XPS, a shoulder denoted C' accompanying the leading main line feature A is clearly resolved. The spectrum for the zigzag chain $SrCuO_2$ closely resembles that of Sr_2CuO_3, whereby the intensity of C' is larger in the former. In addition, referring to Table I, the satellite to main line intensity ratio, I_s/I_m, is larger for $SrCuO_2$ than for Sr_2CuO_3, indicating a larger Δ for the zigzag chain in the language of single-site models. In contrast, for Bi_2CuO_4, Li_2CuO_2, and $Ba_3Cu_2O_4Cl_2$ a comparatively narrow and symmetric main line B is observed at lower binding energy than feature C' in the other 1D cuprates. At the position of feature A either no or small spectral intensity is observed.

The spectrum of $Sr_2CuO_2Cl_2$ has been discussed in more detail elsewhere,[12] The broad main line is composed of two features denoted A and B, and a prominent shoulder C appears at higher binding energies. Compared to $Sr_2CuO_2Cl_2$, the feature B in $Ba_2Cu_3O_4Cl_2$ is much more pronounced. For both 2D systems, I_s/I_m is nearly the same whereas C is positioned at different binding energies. Significantly, the position of feature B is very close to that of the main lines of Bi_2CuO_4, Li_2CuO_2, and $Ba_3Cu_2O_4Cl_2$.

To understand these features we will focus first on the 0D and 1D systems and relate the main line features to the differently coupled CuO_4 units in Bi_2CuO_4, Li_2CuO_2, $Ba_3Cu_2O_4Cl_2$, $SrCuO_2$, and Sr_2CuO_3, assuming the simplified geometry of the Cu-O networks displayed in Fig. 1. In the case of Bi_2CuO_4, the interpretation of the main line spectrum is straightforward: since no coherent planar or linear Cu-O network exists, only a local screening process is possible. Similar arguments can be applied to Li_2CuO_2 as the edge-sharing configuration of the CuO_4 plaquettes with 90° Cu-O-Cu interactions does not support direct oxygen-mediated hole hopping. The hopping processes are instead determined by the small parameter t_{pp}. The similarity of the spectrum of $Ba_3Cu_2O_4Cl_2$ to that of Li_2CuO_2 shows that, despite its more complex structure, the former also represents an essentially 1D chain of edge-sharing plaquettes. Thus in Bi_2CuO_4, Li_2CuO_2, and $Ba_3Cu_2O_4Cl_2$ the Cu $2p$ main line is mostly due to local screening processes, with negligible contribution from the ZRS screening channel or delocalization into O $2p$ band states and can therefore be assigned to a $2p^5 3d^{10}\underline{L}$ final state using the language of single-site models.

Comparing the spectra of Sr_2CuO_3 and $SrCuO_2$ with those of the systems built of edge-sharing plaquettes, it is clear that the former supports *no* locally screened final states (i.e. peak B is missing). This conclusion is supported by recent multiple-site calculations for Sr_2CuO_3 within the three-band d-p model,[19] in which no local screening channel is predicted. Based upon these calculations, feature C' represents a screening channel specific to 1D systems in which one half of the hole density pushed out from the core hole site is transferred to the O sites above and below the Cu core hole site, whereas the rest is situated at the two extremes of the cluster chain due to the large t_{pd} hopping parameter.[19] The intensity of this 1D O $2p$ band screening channel depends on the charge transfer Δ between Cu and O.[19] Finally, we assign feature A to the ZRS screened final state. Although the calculation reproduces the experimental spectrum fairly well, the detailed shape of the main line of the present high-resolution spectrum and the position of C' in particular are not accurately predicted.[20] This emphasizes that, even for this simplest chain system, the frequently used d-p model based upon Cu $3d_{x^2-y^2}$ and O $2p_{x,y}$ orbitals is insufficient and probably has to be extended to include further Cu $3d$ states and the inequivalency of the O sites in the chain.

The dependence upon the coupling path between the CuO_4 plaquettes also offers a simple explanation for the narrow Cu $2p$ main line observed in $NaCuO_2$.[21] In this case, the plaquettes are edge-shared and in light of the data presented here only a locally screened final state would be expected.

As regards the 2D systems, we note first that the main line features B have similar positions to those in Li_2CuO_2, Bi_2CuO_4, and $Ba_3Cu_2O_4Cl_2$ but that additional features A and C appear. Comparing the spectra of $Ba_2Cu_3O_4Cl_2$ and $Sr_2CuO_2Cl_2$ and using arguments analogous to those presented above, we attribute A to the ZRS screened final state and the intensity increase of B compared to A in $Ba_2Cu_3O_4Cl_2$ to the Cu_B site present in the latter. Since Cu_B is connected to the Cu_AO_2 network only via 90° Cu_B-O-Cu_A coupling, the hopping matrix elements are given by t_{pp} and therefore screening will mostly take place locally through the adjacent O sites giving a $2p^5 3d^{10}\underline{L}$ final state. This interpretation is supported by the fact that the difference between the scaled $Ba_2Cu_3O_4Cl_2$ and $Sr_2CuO_2Cl_2$ Cu $2p$ spectra is very similar to those of Bi_2CuO_4, Li_2CuO_2, and $Ba_3Cu_2O_4Cl_2$. The introduction of an extra Cu site appears not to affect the intensity of feature C, which we attribute to a 2D O $2p$ band screening channel.[9,12] For smaller square-planar clusters it has been shown that the final states constituting the O $2p$ band screening channel have little overlap with the O sites neighboring the core hole site and tend to spread over the whole cluster also interacting only weakly with the Cu spins.[9] This justifies the notion of an O $2p$ band screening in two dimensions distinct from the ZRS and local screening channels. The different binding energies of C could be related to the different Cu-O bonding distances of 1.95 Å and 1.99 Å in $Ba_2Cu_3O_4Cl_2$ and $Sr_2CuO_2Cl_2$, respectively, since the energy difference between the ZRS and the O $2p$ band screened final states is expected to depend among other parameters on the hopping energy t_{pd}.

Nevertheless, the large intensity of feature B in $Sr_2CuO_2Cl_2$ (or in the Cu_AO_2 part of the $Ba_2Cu_3O_4Cl_2$ spectrum) remains wholly unexplained within the three-band *d*-*p* model in which the Cu $2p$ main line should consist of only two features with large spectral weight, which would approximately reproduce features A and C in the experiment.[12] An important lesson we derived from the discussion of the much simpler linear chain Sr_2CuO_3 was that the XPS final state is in fact a highly excited state and it is probable that two-hole final states of higher binding energies also have to be considered involving for example apical, i.e. non-planar, orbitals. A recent calculation has shown that out-of-plane interactions can stabilize higher binding energy two-hole states.[22] The probability that these states delocalize depends on the small hopping parameter t_{pp} and thus in accordance with the discussion above, they would lead to a locally screened final state.

In conclusion, we have presented high-resolution Cu $2p$ XPS of 0, 1, and 2D high-quality single-crystalline cuprates in which we distinguish between the locally and non-locally screened contributions to the main lines. In Bi_2CuO_4, Li_2CuO_2, and $Ba_3Cu_2O_4Cl_2$, the main line is essentially due to a locally screened final state. Thus we predict that the lowest electron removal states in these materials will be practically dispersionless in nature. In contrast, we could show that the chain systems based upon corner-sharing CuO_4 plaquettes ($SrCuO_2$, Sr_2CuO_3) display spectral weight due only to nonlocal screening processes, which is in qualitative agreement with calculations within the three-band *d*-*p* model. The spectra of the two dimensional systems ($Sr_2CuO_2Cl_2$, $Ba_2Cu_3O_4Cl_2$) result from a combination of nonlocal screening via ZRS formation and the O $2p$ band, as well as a strong locally screened contribution, in contradiction to calculations. These data represent an ideal experimental basis for the testing of models describing core hole screening in correlated systems.

We gratefully acknowledge discussions with K. Okada and S.-L. Drechsler and thank S. Oswald for generously lending us machine-time. Part of this work is supported by the BMBF (05-605 BDA). The work in Japan is supported by Grants for Priority Area and for COE research from the Ministry of Education, Science, Sports, and Culture.

REFERENCES

[a] Present address: Solid State and Structural Chemistry Unit, Indian Institute of Science, Bangalore 560 012, India

[1] B. O. Wells *et al.*, Phys. Rev. Lett. **74**, 964 (1995)

[2] J. J. M. Pothuizen *et al.*, Phys. Rev. Lett. **78**, 717 (1997)

[3] M. S. Golden *et al.*, Phys. Rev. Lett. **78**, 4107 (1997)

[4] C. Kim *et al.*, Phys. Rev. Lett. **77**, 4054 (1996)

[5] K. Okada and A. Kotani, J. Phys. Soc. Jpn. **58**, 2578 (1989)

[6] G. van der Laan *et al.*, Phys. Rev. B **23**, 4369 (1981)

[7] O. Gunnarsson and K. Schönhammer, Phys. Rev. B **23**, 4315 (1983)

[8] M. van Veenendaal and G. A. Sawatzky, Phys. Rev. Lett. **70**, 2459 (1993)

[9] K. Okada and A. Kotani, Phys. Rev. B **52**, 4794 (1995)

[10] J. M. Tranquada *et al.*, Phys. Rev. B **44**, 5176 (1991)

[11] K. Maiti *et al.*, Europhys. Lett. **37**, 359 (1997)

[12] T. Böske *et al.*, to appear in Phys. Rev. B, Aug. 1 (1997)

[13] for example E. Dagotto and T. M. Rice, Science **271**, 618 (1996)

[14] E. W. Ong *et al.*, Phys. Rev. B **42**, 4255 (1990)

[15] R. Kipka and Hk. Müller-Buschbaum, Z. Anorg. Allgem. Chem. **422**, 231 (1976)

[16] B. J. Suh *et al.*, Phys. Rev. Lett. **75**, 2212 (1995)

[17] R. Kipka and Hk. Müller-Buschbaum, Z. Anorg. Allg. Chem. **419**, 58 (1976)

[18] A. Goldoni *et al.*, Phys. Rev. B **50**, 10435 (1994)

[19] K. Okada *et al.*, J. Phys. Soc. Jpn. **65**, 1844 (1996)

[20] K. Okada, private communication

[21] Mizokawa *et al.*, Phys. Rev. Lett. **67**, 1638 (1991)

[22] R. Raimondi *et al.*, Phys. Rev. B **53**, 8774 (1996)

FIGURES

FIG. 1. Sketch of the Cu-O networks in the different cuprates examined. Cu atoms: •; O atoms: ∘. a) the linear chain in Sr_2CuO_3, b) the zigzag chain in $SrCuO_2$, c) the chain of edge-shared plaquettes in Li_2CuO_2, d) the Cu_AO_2 plane in $Sr_2CuO_2Cl_2$ and the Cu_3O_4 plane in $Ba_2Cu_3O_4Cl_2$ containing an extra Cu_B site (□) and e) the crenellated chains of $Ba_3Cu_2O_4Cl_2$.

FIG. 2. Cu $2p_{\frac{3}{2}}$ photoemission spectra of the single-crystalline cuprates. The 1D chain systems a) $SrCuO_2$, b) Sr_2CuO_3, c) Li_2CuO_2, and d) $Ba_3Cu_2O_4Cl_2$; e) 0D Bi_2CuO_4; planar f) $Sr_2CuO_2Cl_2$and g) $Ba_2Cu_3O_4Cl_2$. Also shown is the difference spectrum g)−f).

TABLES

TABLE I. Features of the Cu $2p_{\frac{3}{2}}$ photoemission spectra of Fig. 2 obtained with a Voigt function fit: included are the binding energies of the different main line features, their full width at half maximum (in brackets), and the ratio of the satellite to the main line intensity I_s/I_m.

Compound	A	B	C'	C	I_s/I_m
Bi_2CuO_4	-	934.1 (1.6)	-	-	0.58[a]
Sr_2CuO_3	933.0 (1.6)	-	934.8 (2.0)	-	0.37
$SrCuO_2$	932.9 (1.4)	-	934.8 (2.2)	-	0.40
Li_2CuO_2	-	934.0 (1.6)	-	-	0.56
$Ba_3Cu_2O_4Cl_2$	-	933.8 (1.1)	-	-	0.62
$Ba_2Cu_3O_4Cl_2$	932.7 (0.8)	933.8 (1.9)	-	935.7 (2.2)	0.50
$Sr_2CuO_2Cl_2$	932.8 (1.0)	933.9 (2.2)	-	936.1 (1.8)	0.52
Difference	-	933.9 (1.2)	-	935.5 (1.5)	0.45

[a] Emission from the Bi 4s core level contributes at about 940 eV, consequently this value is an upper estimate.

T. Böske *et al.*   Fig. 1

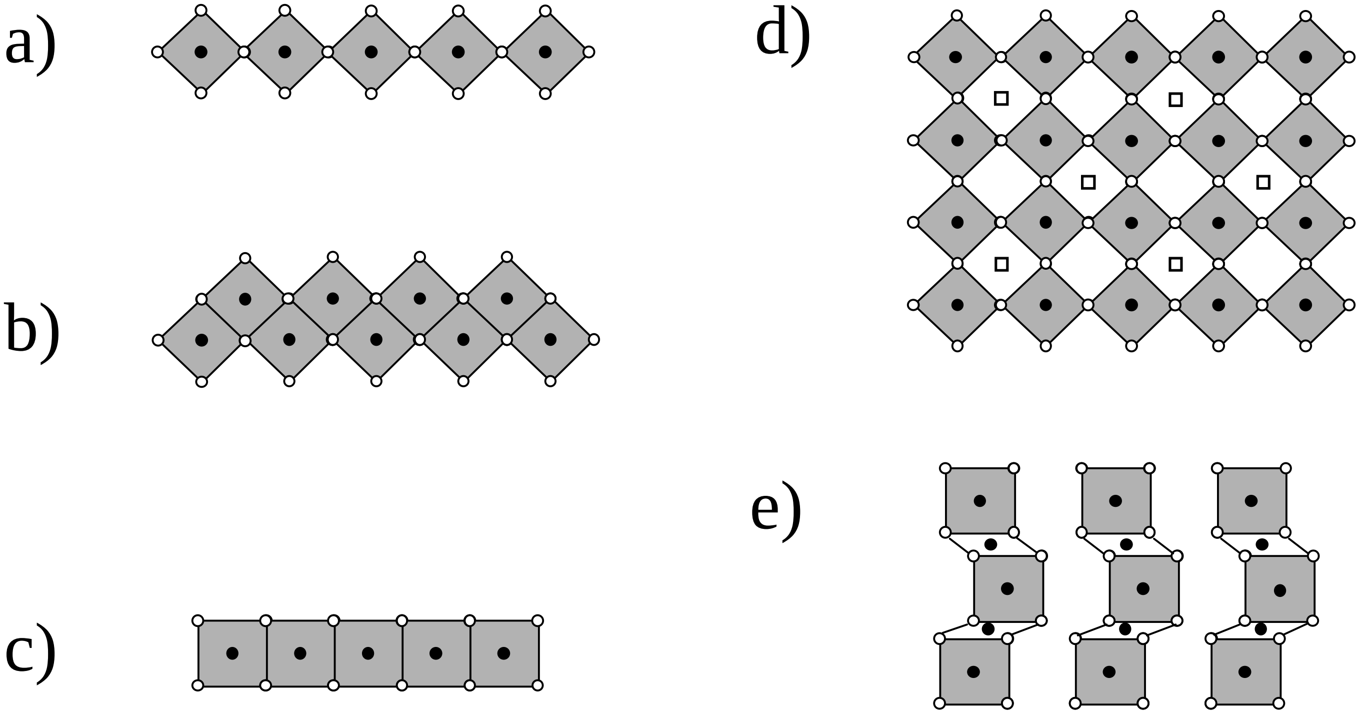

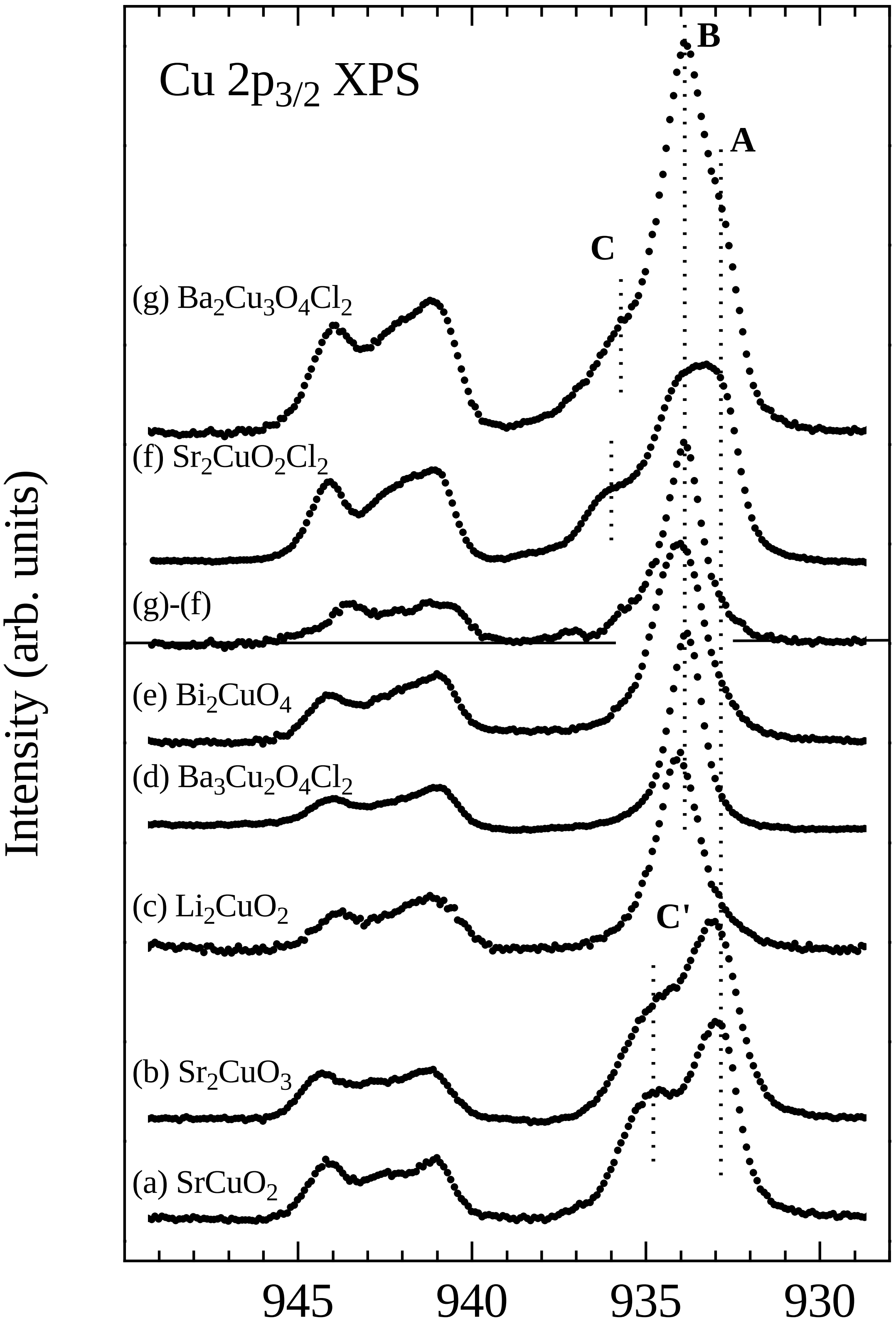
Cu 2p3/2 XPS
B
A
C
C'
(g) Ba2Cu3O4Cl2
(f) Sr2CuO2Cl2
(g)-(f)
(e) Bi2CuO4
(d) Ba3Cu2O4Cl2
(c) Li2CuO2
(b) Sr2CuO3
(a) SrCuO2
Intensity (arb. units)
945
940
935
930
Binding Energy (eV)